LAAS Reference Antennas – Key Siting Considerations

Alfred R. Lopez

BAE SYSTEMS
CNIR Division, Antenna Technology Group
Greenlawn, NY USA

BIOGRAPHY

Alfred R. Lopez is a Life Fellow of the IEEE. He is a Hazeltine Fellow with BAE SYSTEMS Antenna Technology Group. He started his career at Wheeler Laboratories in 1958 as an antenna design specialist. He has made contributions to the theory and practice of electronically scanned antennas. From 1969 to 1990 he was involved with the development of the Microwave Landing System. He has published substantially in IEEE and ION publications, has been issued 39 US Patents, and has received several IEEE and BAE Systems awards.

ABSTRACT

At the ION Annual Meeting, 2003, a paper [1] was presented, which indicated that lateral multipath was a key issue in the overall performance of the LAAS reference antennas at an airport environment. This paper considers two basic types of lateral multipath objects, fixed and transient, that can significantly affect the LAAS performance. The fixed object is the vertical wall (hangars, terminal buildings) that can cause reflection/diffraction multipath from a vertical wall. The transient objects are an aircraft tailfin and an aircraft fuselage. These transient objects have convex surfaces that generate relatively large specular reflection zones with multipath-to-direct signal ratios that can cause significant multipath error.

The goal of this paper is to establish the sensitive zones for these objects. The minimum distance between the reference antenna and the reflecting object will be determined such that the peak multipath error does not exceed a predetermined value. The basic multipath model described in the above referenced paper will be used to quantify the multipath error. In addition, a satellite motion-averaging factor will be considered. The relative motion of the satellite with respect to the earth is such that, in some cases, the multipath interference frequency is well beyond the pass bands of the code delay-lock-loop and 100-second-average filters, and substantial suppression of multipath error is achieved.

INTRODUCTION

Lateral multipath is a key issue in the overall performance of the LAAS reference antennas at an airport environment [1]. Lateral multipath includes all airport objects with the exception of the ground. This paper considers two basic types of lateral multipath objects, fixed and transient, that can significantly affect the LAAS performance. The fixed object is the vertical wall (hangars, terminal buildings) that can cause reflection/diffraction multipath from a vertical wall. The transient objects are an aircraft tailfin and an aircraft fuselage. These transient objects have convex surfaces that generate relatively large specular reflection zones with multipath-to-direct signal ratios that can cause significant multipath error.

An overview of the LAAS Siting Problem is presented in Figure 1. The figure indicates that to satisfy the system accuracy, 63 dB of mitigation is required. After reviewing the general definition of lateral multipath, the general characteristics of a vertical wall, and aircraft tailfins and fuselages are described. The overall LAAS multipath system error is described via a flow diagram, starting with the direct and indirect (multipath) signals, and ending with the system error at the output port of the 100-second-average post filter of the receiver. The concept of mujltipath satellite motion averaging is described. A critical zone is described as the location of all possible reflectors with delays that are less than one chip (293 meters). Finally, sensitive zones are described for a vertical wall and the 747 aircraft tailfin. These are the locations for these objects that can possibly cause excessive error.

LAAS Siting Problem -- Overview

	Multipath Mitigation Factor	
	Min	Max
Nominal Multipath Peak Error, 147m (1/2 Chip)	0 dB	0 dB
Receiver Processing, Narrow (0.1) Correlator	-20 dB	–40 dB
Post Filters, Satellite Motion Averaging	-0.0 dB	–36 dB
Maximum Permissible M/D Ratio	-43 dB	<0 dB
Maximum Permissible Multipath Error, 0.1m	-63 dB	–63 dB

For a particular multipath object the minimum distance between the object and the reference antenna is determined such that the M/D ratio does not exceed the value indicated.

Figure 1

LATERAL MULTIPATH OBJECTS

An overview of airport multipath is presented in Figure 2. In general, lateral multipath is defined as all airport multipath excluding the local ground about the reference antenna. The key lateral multipath objects, with regard to siting considerations for the LAAS reference antennas, are vertical walls, such as hangar walls or hangar doors, and aircraft tailfins and fuselages. Aircraft surfaces are particularly bothersome because they are transient. An aircraft can taxi and park at a location and cause a significant multipath error that could affect more than one of the reference antennas. The net result could be the loss of the availability of a satellite. This would impact the overall system availability.

Airport Multipath

- Local Ground
- Lateral Multipath
  - Hangars
  - Aircraft Tailfin
  - Aircraft Fuselage
  - Airport Control Tower
  - Terminal Buildings
  - Buses
  - Maintenance Vans
  - Surrounding Skyline

Figure 2

VERTICAL WALL MULTIPATH

The basic geometry for the reflection and shadow zones associated with a vertical wall is shown in Figures 3 and 4.

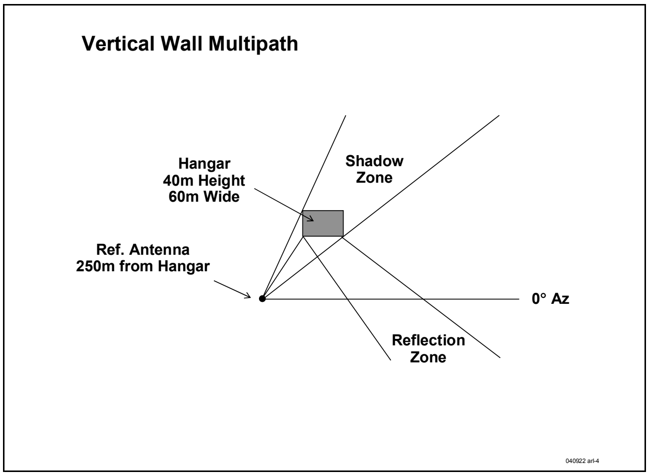

Figure 3

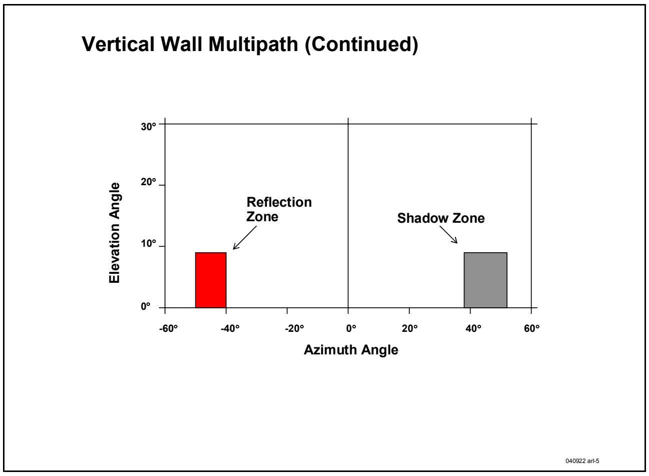

Figure 4

Figure 3 is a plan view showing the reflection zone for one wall of the hangar and the shadow zone caused by two walls. Figure 4 shows the possible extent of the reflection and shadow zones in azimuth and elevation angle space.

Figure 5

AIRCRAFT TAILFINS AND FUSELAGES

Photographs of a 747 tailfin and fuselage are shown in Figure 5. These are large, mostly convex metal, surfaces that can cause significant multipath over fairly large angular zones. Some typical angular extent of these reflection zones is indicated in Figure 6. (The 747 fuselage actually has a concave reflecting surface at the intersection of the upper deck and the main fuselage. This could significantly enhance the reflection with respect to the reflection of a normally convex surface.)

Typical Angular Extent of Reflection Zones

Multipath Object (Antenna to object distance is 250m. Antenna height above ground is 3m)	Angular Extent (Degrees)	
	Azimuth	Elevation
Vertical Wall	±5	0 to 10
747 Aircraft Tailfin	±15	5 to 15
747 Aircraft Fuselage	±20	0 to 90

040922 arl-7

Figure 6

LAAS MULTIPATH SYSTEM ERROR

A flow diagram for the LAAS multipath system error is presented in Figure 7. The top five layers present an analysis plan for quantifying the multipath-to-direct, M/D, signal ratio. The basic approach for this analysis was developed during the development of the Microwave Landing System [2] [3]. This approach incorporates four multiplicative factors to provide estimates of the M/D ratio. It should be helpful in supporting the LAAS siting effort, which has been ongoing for several years. [4] [5]. Figure 8 shows some possible factors and the resulting M/D ratios.

The receiver processing factor has been characterized by Braasch [6] [7]. Appendix A indicates that -20dB is a representative upper bound for the autocorrelation sidelobe factor. For a 0.1 receiver correlator spacing the total sidelobe multipath suppression factor is 40dB. With a peak raw error of 147m, the sidelobe error at the output of the receiver is 1.5m. Obviously, multipath objects in the sidelobe region need to be considered.

Further suppression of multipath error is provided by satellite motion averaging. Figure 9 presents the concept. A multipath source will produce constant phase contours in angle space whose spacing depends on the distance between the multipath source and the reference antenna.

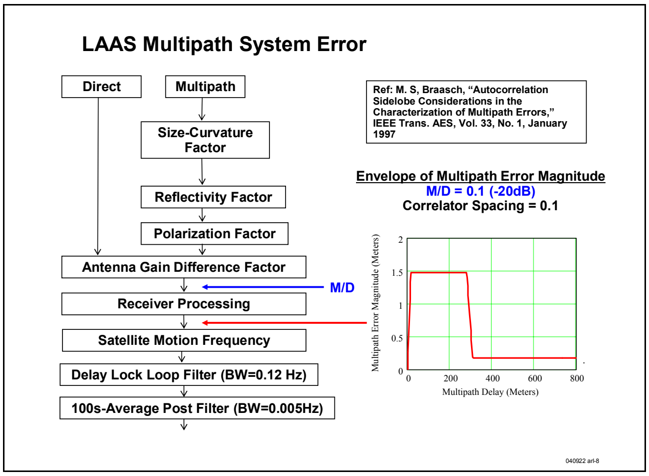

Figure 7

Example Multipath Factors

Factor	Vertical Wall Hor	Vertical Wall Vert	Aircraft Tailfin Hor	Aircraft Tailfin Vert	Aircraft Fuselage Hor	Aircraft Fuselage Vert
Size or Curvature (Whichever Is Smaller)	1	1	1	1	1	1
	1	1	0.15	1	1	0.06
Reflectivity	0.5		1		1	
Polarization (Linearly Polarized Ant.)	1		1		1	
Antenna Gain	1		0.7		0.7	
M/D	0.5 (-6.0dB)		0.11 (-19.6dB)		0.04 (-27.8dB)	

Note: The size-curvature factor is the product of the horizontal and vertical components.

040922 arl-9

Figure 8

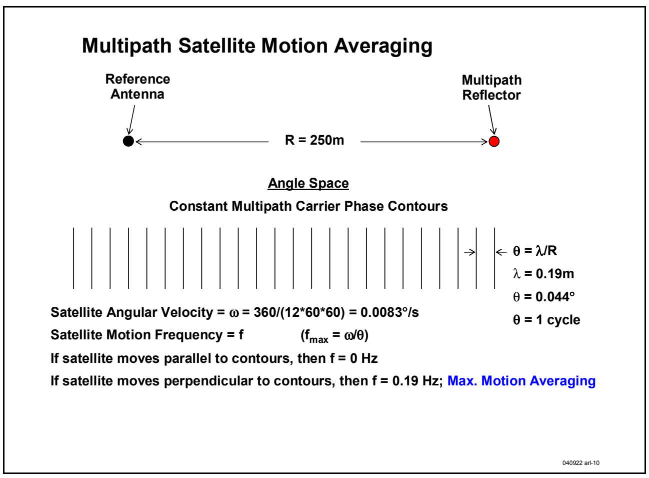

Figure 9

If the satellite motion is perpendicular to the contour lines, then the multipath signal will have a frequency that is shifted from the carrier frequency. This frequency difference is equal to the satellite angular velocity divided by the angle between the constant phase contours. This frequency shift can be beyond the pass band of the delay-lock-loop filter and well beyond the pass band of the 100-second average post filter. The reduction in the multipath error can be substantial.

If the satellite motion is parallel to the constant phase contours, then there is no frequency shift and no corresponding suppression of the multipath error. It is recommended that in a general multipath analysis, the satellite motion averaging factor be set to unity. For site-satellite specific situations, the satellite motion averaging should be quantified. An example is presented later in the paper.

THE FRESNEL UNIT OF LENGTH

The Fresnel Unit, FU, of length is here defined as $\mathbf{FU} = \sqrt{R\lambda}$ (see Figure 10). In general, the distance, R, is an effective distance that is equal to $(R_1R_2)/(R_1 + R_2)$, where R_1 is the distance from the antenna to the reflecting object, and R_2 is the distance from the reflecting object to the satellite. For the case under consideration, $R_2 >> R_1$, and $R = R_1$.

The Fresnel Unit Of Length

Fresnel Unit = FU = $\sqrt{R\lambda}$
R = Multipath Reflector to Antenna Distance
λ = Carrier Freespace Wavelength

If reflecting object size is comparable or larger than FU, then the object has the potential to cause a multipath-to-direct, M/D, ratio near unity (0 dB).

If reflecting object is small with respect to FU, then the M/D ratio is less than unity, and the maximum possible M/D ratio is given by the equation:

$$\frac{M}{D} = \frac{A}{FU^2} \quad \text{(Voltage Ratio)}$$

A = Reflector Projected Area

040922 arl-11

Figure 10

The Fresnel Unit of length serves as a measure of the potential of a reflecting object to cause large or small M/D ratios. As noted in the Figure 10, if the reflecting object size is comparable or larger than the Fresnel Unit, then the object has the potential to cause an M/D ratio near unity. If the reflecting object is small with respect to the Fresnel Unit, then the object will have an M/D ratio that is less than unity. The Fresnel Unit can be used to separate the strong from the weak reflectors.

Figure 10 presents an equation that shows the relationship between M/D, reflector projected area, A, and the FU, when the object size is less than the FU. Figure 11 presents a derivation of this equation.

Derivation Of Multipath Formula For Small Flat Reflector

P = Power p = Power Density G = Antenna Gain A = Projected Area

$$p_{Direct} = \frac{P * G_{Direct}}{4\pi R_0^2} \qquad p_{Reflected} = \frac{P * G_{Reflected}}{4\pi R_1^2}\,\frac{A * 4\pi A/\lambda^2}{4\pi R_2^2}\left[\frac{R_1+R_2}{R_1+R_2}\right]^2$$

$$R = \frac{R_1R_2}{R_1+R_2} \qquad p_{Reflected} = \frac{P * G_{Reflected}}{4\pi(R_1+R_2)^2}\,\frac{A^2}{R^2\lambda^2}$$

$$\frac{p_{Reflected}}{p_{Direct}} = \frac{G_{Reflected}}{G_{Direct}}\left[\frac{R_0}{R_1+R_2}\right]^2\left[\frac{A}{R\lambda}\right]^2$$

$$\frac{M}{D} = \frac{V_{Reflected}}{V_{Direct}} = \sqrt{\frac{G_{Reflected}}{G_{Direct}}}\,\frac{R_0}{R_1+R_2}\,\frac{A}{R\lambda} \qquad \frac{A}{R\lambda} = \frac{W}{\sqrt{R\lambda}}\,\frac{H}{\sqrt{R\lambda}}$$

Gain Factor — **Distance Factor** — **Size Factor** — **Size Factors: Horizontal, Vertical**

040922 arl-12

Figure 11

In Figure 11, the reflector is a flat perfect electric-conducting plate with a projected square area, A, that is D units on a side. The antenna is in the far-field of the plate.

$$R > \frac{2D^2}{\lambda}, \text{ or } \frac{1}{2} > \frac{A}{R\lambda}$$

For the case being considered the gain and distance factors are equal to one. R_0 is the direct distance between transmit and receive antennas. For the basic multipath model [1] [2] the reference reflector is a perfect mirror that is tangent to the reflecting object at the point of reflection. The gain and distance factors in Figure 11 correspond to the case of the perfect mirror, an infinitely large, perfect electric-conducting plate.

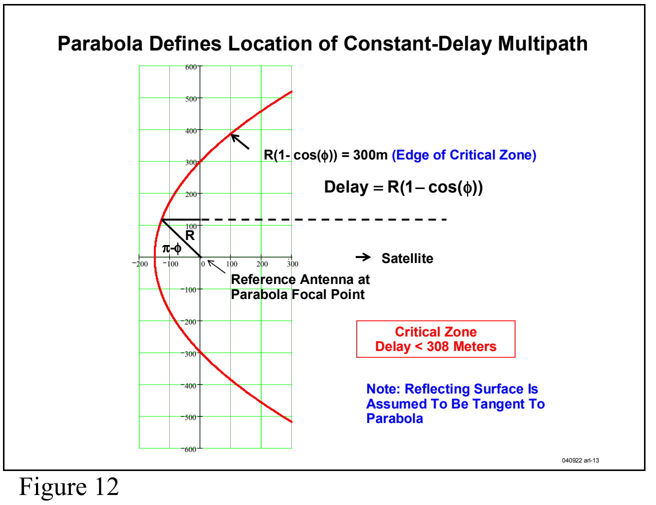

Figure 12

THE CRITICAL ZONE

The surface of constant delay between two points is an ellipsoid. If one focal point of the ellipsoid is at infinity, then the surface is a paraboloid. For the case of a satellite at a low elevation angle, the intersection of a paraboloid and the ground plane is essentially a parabola.

In this paper the critical zone is defined as the location of reflecting objects whose delay is less than 308 meters (1.05 chips). In this zone the receiver processing factor is equal to the correlator spacing. It is -20dB for a correlator spacing of 0.1. Outside of this zone it is typically less than -40dB for the same correlator spacing (see Appendix A).

Heretofore [18] it was generally accepted that multipath objects outside the critical zone do not pose a significant threat. In Appendix A, it is shown that the autocorrelation sidelobes are typically more than 20dB down from the peak of the correlation function. In combination with a 0.1 correlator spacing, the total sidelobe suppression of the peak error is 40dB. For the 293m chip, the resulting sidelobe peak error is 1.5m. Clearly, this level of multipath error is not acceptable and must be considered in a site analysis.

SENSITIVE ZONE

In this paper the sensitive zone is defined as the region surrounding the reference antenna where a particular multipath source has the potential (size, distance and alignment) to cause an error that exceeds 0.1 meters.

Vertical Wall

Using the model developed in [2] it is possible to estimate the M/D for the case of the vertical wall. The size factor is the product of horizontal-plane and vertical-plane factors. These size factors are presented in Figure 13.

Size Factor Equations – Vertical Wall

Horizontal Size Factor (Reflection at Center of Azimuth Zone)

$$\rho_{Hor} = \frac{W \sin(\phi/2)}{\sqrt{R\lambda}}$$

W = Width of Reflector

ϕ = Reflector Azimuth Angle

R = Reflector to Antenna Distance

If $\rho_{Hor} < 1$, Then $\rho_{Hor} = \rho_{Hor}$, Else $\rho_{Hor} = 1$

Size Factor

$$\rho_{Size} = \rho_{Hor}\rho_{Vert}$$

Vertical Size Factor (Top Edge Reflection/Diffraction)

$$\rho_{Vert} = \frac{\sqrt{R\lambda}}{2\pi h}$$

$h = R\tan(\theta) - H$ = Distance Between Line-of-Sight and Top Edge of Wall

H = Height of Reflector

θ = Satellite Elevation Angle

If $\rho_{Vert} < 1$ and $h > 0$, Then $\rho_{Vert} = \rho_{Vert}$, Else $\rho_{Vert} = 1$

040922 ari-13

Figure 13

The horizontal factor corresponds to the M/D at the center of the reflection zone for a vertical strip that has a width equal to W. The vertical factor corresponds to the M/D for a knife edge that has a height above the reference antenna equal to H. The vertical factor varies with the satellite elevation angle. It is noted that the size factor has a sin(ϕ/2) projected-area dependence (satellite reflection alignment), which has a modified cardioid ($\sqrt{\text{cardioid}}$) pattern in the azimuth plane.

Sensitive Zone Factors – Vertical Wall

	Reflector Location: Inside Critical Zone	Reflector Location: Outside Critical Zone
Maximum Error	147m	
Receiver Processing Factor	0.10	0.01
Reflector Reflectivity Factor	0.25	
Reduced Error	3.7m	0.37m
Maximum Allowable Error	0.10m	
Required Size Factor	0.027 (-31.4dB)	0.27 (-11.4dB)

040922 ari-15

Figure 14

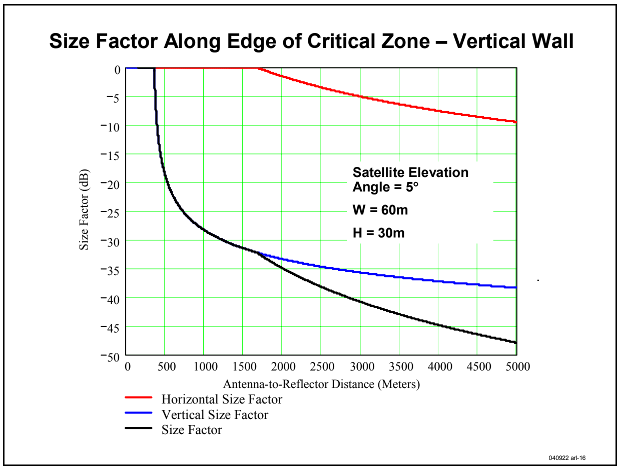

Figure 15

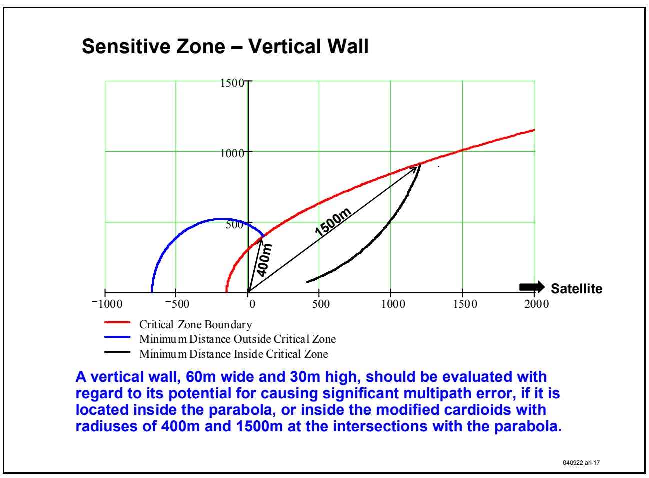

Figure 16

Figure 14 indicates that to satisfy the 0.1m error tolerance the size factor has to be less than -31.4dB inside the critical zone and less than -11.4dB outside the critical zone. Figure 15 shows the variation of the size factor along the boundary of the critical zone. This information is used to map out the edge of the sensitive zone for the vertical wall as shown in Figure 16.

Size Factor & Curvature Factor Equations – 747 Tailfin

Size Factors (Satellite at Center of Reflection Zone)

$$\rho_{Hor\ Size} = \frac{W \sin(\phi/2)}{\sqrt{R\lambda}} \qquad \rho_{Vert\ Size} = \frac{H}{\sqrt{R\lambda}}$$

W = Reflector Width

H = Reflector Height

ϕ = Reflector Azimuth Angle

R = Reflector to Antenna Distance

If $\rho_{Size} < 1$, Then $\rho_{Size} = \rho_{Size}$, Else $\rho_{Size} = 1$

Horizontal Curvature Factor

$$\rho_{Curv} = \frac{1}{\sqrt{1 + \frac{2R}{r \sin(\phi/2)}}}$$

r = Reflector Radius of Curvature

Horizontal Size-Curvature Factor

If $\rho_{Hor\ Size} < \rho_{Curv}$ Then $\rho_{Hor\ Size\text{-}Curv} = \rho_{Hor\ Size}$ Else $\rho_{Hor\ Size\text{-}Curv} = \rho_{Curv}$

040922 art-18

Figure 17

Size-Curvature Equation Validation

$$\rho_{Size\text{-}Curvature} = \rho_{Horizontal\ Size\text{-}Curvature}\ \rho_{Vertical\ Size}$$

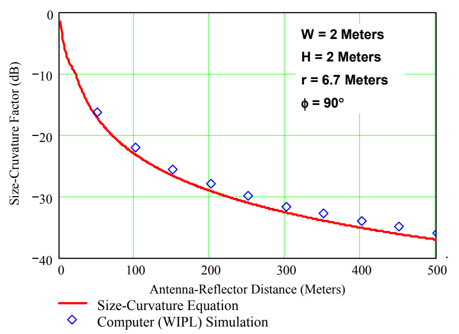

040922 art-18

Figure 18

747 Tailfin

The tailfin of a 747 aircraft is estimated to be about 9m wide by 9m high. It has curvature in the horizontal plane with a radius of curvature of about 30m [2]. Since it is a metallic surface the reflectivity factor is equal to one. Also, it is assumed that the reference antenna has linear polarization, and consequently, the polarization factor is also equal to one [1]. The size factor and curvature factor equations are presented in Figure 17. The horizontal size and curvature factors are inherently related. The horizontal size-curvature factor is equal to the smaller of the two factors. This relationship was validated using a computer simulation, the results of which are shown in Figure 18

Sensitive Zone Factors – 747 Tailfin

	Reflector Location: Inside Critical Zone	Reflector Location: Outside Critical Zone
Maximum Error	147m	
Receiver Processing Factor	0.10	0.01
Antenna Gain Factor	0.7	
Reflector Reflectivity Factor	1.0	
Reduced Error	10.3m	1.03m
Maximum Allowable Error	0.10m	
Required Size-Curvature Factor	0.0097 (-40.3dB)	0.097 (-20.3dB)

040922 art-20

Figure 19

Size-Curvature Factor Along Edge of Critical Zone – 747 Tailfin

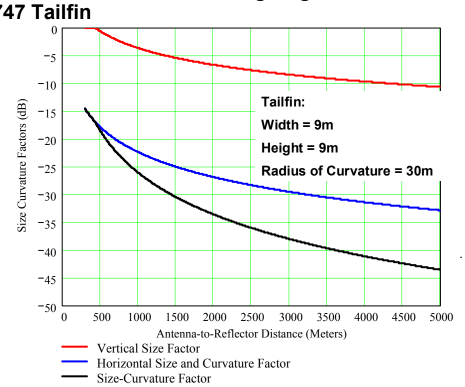

040922 art-20

Figure 20

Sensitive Zone – 747 Tailfin

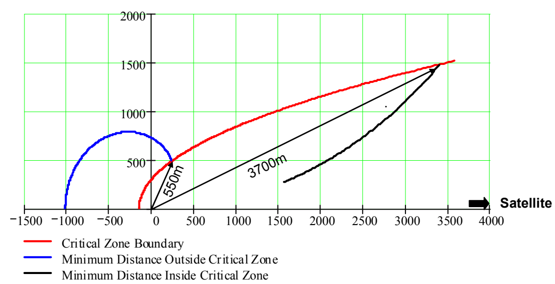

A 747 tailfin should be evaluated with regard to its potential for causing significant multipath error, if it is located inside the parabola or inside the modified cardioids with radiuses of 550m, and 3700m at the intersections with the parabola.

040922 art-22

Figure 21

In Figure 18 the geometry was set such that the curvature factor was the smaller of the two factors. Computer simulations were also run for the cases when the size factor was the smaller of the two and when they were about equal. In all cases there was good agreement between the equations of Figure 17 and the computer simulations.

Figure 19 indicates that to satisfy the 0.1m error tolerance the tailfin size-curvature factor has to be less than -40.3dB inside the critical zone and less than -20.3dB outside the critical zone.

Figure 20 shows the variation of the size-curvature factor along the boundary of the critical zone. This information is used to map out the edge of the sensitive zone for the tailfin as shown in Figure 21.

POLARIZATION AND MOTION AVERAGING FACTORS

The indicated sensitive zones for the vertical wall and aircraft tailfin are very large, and in many cases, would seriously impact the siting of reference antennas. As noted in [1], a reference antenna with right hand circular polarization with an axial ratio of 2 dB would provide about another 20 dB reduction of the M/D ratio. This would greatly reduce the size of the sensitive zones.

It is noted that the satellite motion frequency depends directly on the separation distance, R, between the antenna and the reflecting object and, consequently, increased satellite-motion-averaging suppression of multipath error is directly related to the separation distance. An example is presented below that illustrates the multipath suppression related to satellite motion averaging.

It is assumed that the satellite angular velocity component perpendicular to the multipath constant-phase contours is one half the satellite angular velocity, and the spacing of the contours is twice the minimum spacing. The frequency dependence on R is given by the equation:

$$f(R) = \frac{1}{4}\,\frac{2\pi}{12(60)(60)}\,\frac{R}{\lambda}\ \text{(Hz)}$$

The phase lock loop filter is assumed to be a low-pass single-pole filter with a pass-band frequency, f_1 = 0.12 Hz. The filter response, $F_1(R)$, is approximated by:

$$\text{If } \frac{f_1}{f(R)} < 1, \text{ Then } F_1(R) = \frac{f_1}{f(R)}, \text{ Else } F_1(R) = 1$$

The 100s averaging filter is assumed to be a low-pass single-pole filter with a pass-band frequency, f_2 = 0.005 Hz. The filter response, $F_2(R)$, is approximated by:

$$\text{If } \frac{f_2}{f(R)} < 1, \text{ Then } F_2(R) = \frac{f_2}{f(R)}, \text{ Else } F_2(R) = 1$$

Figure 22 presents the size-motion multipath suppression factor along the critical zone perimeter. As compared with Figure 16, Figure 23 indicates that with the satellite motion averaging factor included the sensitive zone is greatly reduced. In Figure 23 the sensitive zone is bounded by the critical zone parabola and a modified cardioid with a 400m-radius at the intersection with the parabola.

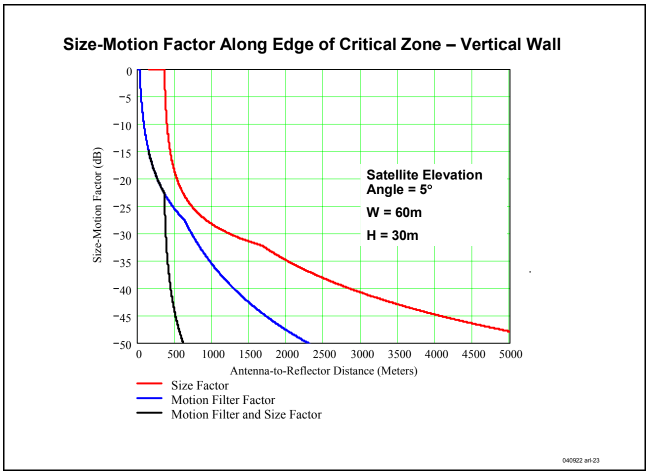

Figure 22

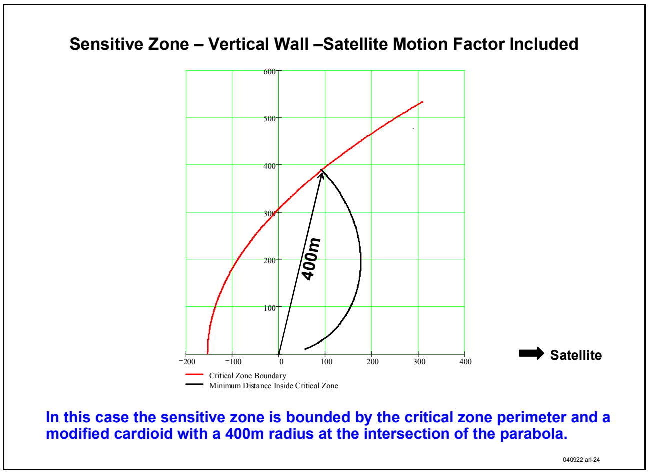

Figure 23

MATH MODELING

The airport environment is complicated and varied, so much so, that no one particular math model is useful in all situations. Specially designed software [5] and commercially available software packages can be used to accurately predict M/D and, receiver processing and filtering. These models are generally more useful for either the case when the object is electrically large or when the object is electrically small. In all cases, the math models can not typically accommodate all of the features of the airport objects and, consequently, there is some residual error in the performance predictions.

The model originally developed in [2], and further refined in [1] and in this paper, is universally applicable to large and small objects. It is based on analysis and the decomposition of the problem to its basic elements. It provides insight into the phenomena that affect the M/D ratio. It also provides a relatively simple way for estimating peak M/D ratios.

One particularly useful feature of this simple model is the curvature factor, which provides a way of quickly estimating the magnitude of reflections off convex aircraft surfaces. The curvature factor defined in [2] was first derived by Riblet and Barker [9] as a divergence factor for a doubly curved surface. The author converted their results to the form presented in Figure Q-13 (a) of [2], where the reference reflector is a perfect electric mirror.

A siting engineer will need all of the tools available. A siting handbook should incorporate computer software packages, both custom and commercial, and the concepts and methodology described in this paper.

SUMMARY

- Vertical walls, aircraft tailfins and aircraft fuselages have been identified as key multipath sources that need special consideration in the siting of the LAAS reference antennas.
- Multipath satellite motion averaging was described. It is very effective in suppressing multipath error however it is recommended that the basic analysis be performed independent of the motion averaging factor. This will provide insight into the basic error mechanism.
- A critical zone was defined as the region around the reference antenna were the multipath delays are less than 1.05 chips, 308 meters. A parabola defines the outer boundary of this region.
- A sensitive zone was defined as a region where lateral multipath objects have the potential to cause excessive error. The sensitive zones for a vertical wall and a 747 aircraft tailfin were evaluated.
- The goal was to introduce a relatively simple methodology for quantifying the potential threat associated with common airport multipath sources.

ACKNOWLEDGEMENTS

The author would like to thank Dr. Michael S. Braasch, of Ohio University, for his help in characterizing the autocorrelation sidelobe factor and for his general encouragement of the work reported in this paper.

APPENDIX A – Autocorrelation Sidelobe Factor

Via [10] the following data (PRN Number, Sidelobe Error Factor) were provided:

(1, 0.0) (2, 0.0625) (3, 0.0625) (4, 0.0625) (5, 0.0) (6, 0.0625) (7, 0.0667) (8, 0.1176) (9, 0.0625) (10, 0.0625) (11, 0.0625) (12, 0.0) (13, 0.0625) (14, 0.0) (15, 0.0667) (16, 0.0625) (17, 0.0667) (18, 0.1250) (19, 0.1250) (20, 0.0625) (21, 0.0667) (22, 0.0588) (23, 0.0625) (24, 0.1333) (25, 0.1250) (26, 0.0) (27, 0.0625) (28, 0.0625) (29, 0.0) (30, 0.1250) (31, 0.0) (32, 0.0)

This data has the following characteristics:
Maximum Value = 0.1333 (-17.5 dB)
Mean Value = 0.0590 (-24.6 dB)
Standard Deviation = 0.0420 (-27.5 dB)
Root Mean Square Value = 0.0721 (-22.8 dB)
Mean + Standard Deviation = 0.1010 (-19.9 dB)

The mean value plus the standard deviation (-20 dB) is a value that is not exceeded more than 16 percent of the time, and is used in this paper as representative of the upper bound for the autocorrelation sidelobe factor.

REFERENCES

[1] A. R. Lopez, "LAAS Reference Antennas – Circular Polarization Mitigates Multipath Effects," Proc. Of ION Annual Meeting, Albuquerque, NM, June 23-25, 2003

[2] H. A. Wheeler, A. R. Lopez, "Multipath Effects in Doppler MLS," Multipath Section of Hazeltine Report 10926, "Five Year Microwave Landing System Development Program Plan," September 1972; Hazeltine Reprint H-222; October 1974.

[3] A. R. Lopez, "Scanning-Beam Microwave Landing System – Multipath-Errors and Antenna-Design Philosophy," IEEE Transaction on Antennas and Propagation, vol. AP-25, No. 3, 1977

[4] D. Lamb, "Development of Local Area Augmentation System Siting Criteria," ION 57th Annual Meeting/CITGTF 20th Biennial Guidance Test Symposium, 11-13 June 2001, Albuquerque, NM.

[5] J. M. Kelly, J.C. Cohenour, M. F. DiBenedetto, D. Lamb, "An Advanced Multipath Model for DGPS Reference Site Analysis," ION 60th Annual Meeting, June 7-9, 2004, Dayton, OH.

[6] M. S. Braasch, "Autocorrelation Sidelobes Considerations in the Characterization of Multipath Errors," IEEE Trans. AES, Vol. 33, No. 1, January 1997

[7] M. S. Braasch, M. F. DiBenedetto, "Spread-Spectrum Ranging Multipath Model Validation," IEEE Trans. AES, Vol. 37, No. 1 January 2001

[8] D. B Thornberg, D. S. Thornberg, M. F. DiBenedetto, M. S. Braasch, F. van Graas, C. Bartone, "LAAS Integrated Multipath-Limiting Antenna," Navigation, ION Journal, Vol. 50, No. 2, Summer 2003.

[9] H. J. Riblet, C. B. Barker, "A General Divergence Formula," Journal of Applied Physics, Vol. 19 pp. 63-70, January 1948.

[10] M. S. Braasch, Email correspondence, August 7, 2004.